Available online at www.sciencedirect.com
SCIENCE DIRECT®
PERGAMON
Polyhedron 22 (2003) 1783–1788
POLYHEDRON
www.elsevier.com/locate/poly

New example of Jahn-Teller isomerism in $[Mn_{12}O_{12}(O_2CR)_{16}(H_2O)_4]$ complexes

Mònica Soler [a], Wolfgang Wernsdorfer [b,*], Ziming Sun [c], Daniel Ruiz [c], John C. Huffman [d], David N. Hendrickson [c,*], George Christou [a,*]

[a] Department of Chemistry, University of Florida, Gainesville, FL 32611-7200, USA
[b] Laboratoire Louis Néel-CNRS, BP 166, 25 Avenue des Martyrs, 38042 Grenoble Cedex 9, France
[c] Department of Chemistry, University of California at San Diego, La Jolla, CA 92093-0358, USA
[d] Molecular Structure Center, Indiana University, Bloomington, IN 47405-4001, USA

Received 6 October 2002; accepted 14 January 2003

Abstract

The isolation and characterization of a new pair of Jahn-Teller isomers of $[Mn_{12}O_{12}(O_2CCH_2Bu^t)_{16}(H_2O)_4]$ (**3**) are reported: complex $\mathbf{3}\cdot CH_2Cl_2\cdot MeNO_2$ (**3a**) and $\mathbf{3}\cdot CH_2Cl_2\cdot MeCN$ (**3b**). These Jahn-Teller isomers have been crystallized in the same triclinic space group, and differ only in one abnormally oriented Jahn-Teller axis in **3a** and in the identity of one solvent molecule of crystallization. Magnetic data show much faster magnetization relaxation for **3a** (the low-temperature, LT, form) compared with **3b** (the high-temperature, HT, form), exhibiting a peak in the out-of-phase magnetic susceptibility in the 2–4 and 5–7 K ranges, respectively. Magnetization vs. DC field scans on aligned crystals of **3a** and **3b** display hysteresis with coercivities that vary with temperature, as expected for single-molecule magnets. The hysteresis loops also exhibit the step features that are the signature of quantum tunneling of magnetization.

Keywords: Single-molecule magnets; Hysteresis; Jahn-Teller isomers; Quantum tunneling of magnetization

1. Introduction

In 1993, it was discovered that $[Mn_{12}O_{12}(O_2CMe)_{16}(H_2O)_4]\cdot 4H_2O\cdot 2MeCO_2H$ (**1**), abbreviated as Mn_{12}ac, functions as a nanoscale magnet at temperatures below its blocking temperature (T_B) [1]. Such single-molecule magnets (SMMs) have since attracted considerable attention. There are two main reasons for this recent interest. First, SMMs offer the possibility of future technological applications, such as for very high-density information storage, where each molecule would store one bit of information. Second, owing to their sub-nanoscale dimensions, as well as monodisperse particles, they can help to bridge the gap between the quantum and classical understanding of magnetism. In 1996, quantum tunneling of magnetization (QTM) was observed in a sample of complex **1** [2]. Since then, small variations of the $[Mn_{12}O_{12}(O_2CR)_{16}(H_2O)_4]$ core and environment have been shown to significantly affect the hysteresis plots and the quantum tunneling behaviour. For example, there are both slower- and faster-relaxing forms of the Mn_{12} complexes, and these have been shown to be due to two isomeric forms of the $[Mn_{12}O_{12}]^{16+}$ core, involving different relative orientations of the Mn^{III} Jahn-Teller elongation axes. We have called this "Jahn-Teller isomerism" [3]. In 2001, two Jahn-Teller isomers for the same Mn_{12} complex were isolated and characterized, $[Mn_{12}O_{12}(O_2CC_6H_4\text{-}p\text{-}Me)_{16}(H_2O)_4]\cdot 3H_2O$ (**2a**) and $[Mn_{12}O_{12}(O_2CC_6H_4\text{-}p\text{-}Me)_{16}(H_2O)_4]\cdot HO_2CC_6H_4\text{-}p\text{-}Me$ (**2b**) [4]. In this case, the two forms crystallized in different space groups with consequently significantly different environments around the molecules. We now report the isolation and characterization of a second pair of Jahn-Teller isomers for the $[Mn_{12}O_{12}(O_2CCH_2Bu^t)_{16}(H_2O)_4]$ (**3**) complex. In this case, both structures are in the same space group, with almost identical environments, em-

* Corresponding authors. Fax: +33-76-87-50-60.
E-mail address: wernsdor@polyenrs-gre.fr (W. Wernsdorfer).

0277-5387/03/$ - see front matter © 2003 Elsevier Science Ltd. All rights reserved.
doi:10.1016/S0277-5387(03)00260-2

phasizing the small energy difference between JT isomers. The preparation, structures and magnetic properties of the two forms are described.

2. Results and discussion

$[Mn_{12}O_{12}(O_2CCH_2Bu^t)_{16}(H_2O)_4]$ (**3**) was obtained by carboxylate substitution of $[Mn_{12}O_{12}(O_2CMe)_{16}(H_2O)_4]$ (**1**) with $Bu^tCH_2CO_2H$ in toluene [5]. Several cycles of treatment with $Bu^tCH_2CO_2H$ were needed to ensure replacement of all the acetate ligands. The final crystallization was from $CH_2Cl_2/MeNO_2$. AC magnetic susceptibility studies on crystals maintained in mother liquor show one frequency-dependent peak in the out-of-phase (χ''_M) plot in the 2–4 K region for oscillation frequencies up to 1500 Hz, characteristic of a faster-relaxing species. Normal, slower-relaxing Mn_{12} complexes exhibit χ''_M peaks in the 5–7 K range. In Fig. 1 is presented a time dependence study of the out-of-phase (χ''_M) AC susceptibility peaks showing conversion from a pure sample of the low-temperature (LT) form to essentially only the high-temperature (HT) form. In this study, crystals of **3a** were removed from mother liquor and their χ''_M responses were monitored with time as they slowly lost the lattice solvent. These two forms have been crystallographically characterized as $[Mn_{12}O_{12}(O_2CCH_2Bu^t)_{16}(H_2O)_4]\cdot CH_2Cl_2\cdot MeNO_2$ (**3a**) and $[Mn_{12}O_{12}(O_2CCH_2Bu^t)_{16}(H_2O)_4]\cdot CH_2Cl_2\cdot MeCN$ (**3b**), for the LT and HT form, respectively.

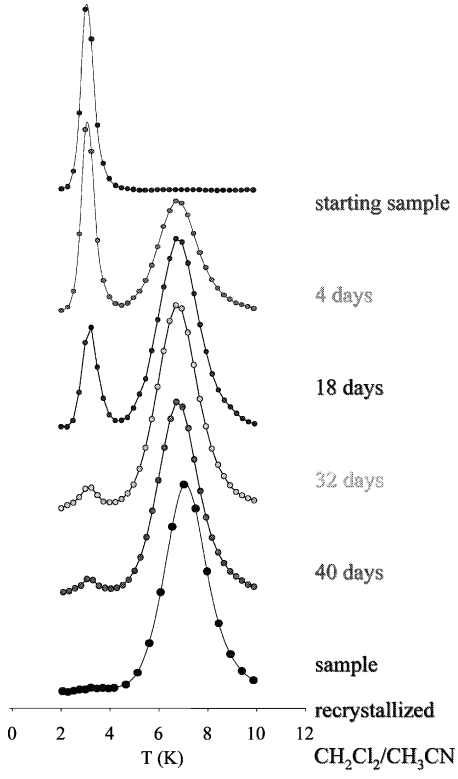

Fig. 1. Time-dependent out-of-phase (χ''_M) AC magnetic susceptibility signal; conversion from the fast-relaxation process (seen in complex **3a**) to the slow-relaxation process (seen in complex **3b**).

2.1. X-ray structures

Single crystals of $[Mn_{12}O_{12}(O_2CCH_2Bu^t)_{16}(H_2O)_4]\cdot CH_2Cl_2\cdot MeNO_2$ (**3a**) were obtained from $CH_2Cl_2/MeNO_2$. A PovRay plot of **3a** is presented in Fig. 2. Complex **3a** crystallizes in the triclinic space group $P\bar{1}$ with two Mn_{12} molecules in the unit cell, as well as two CH_2Cl_2 and two $MeNO_2$ molecules. The complex has the same structure as previously characterized $[Mn_{12}O_{12}(O_2CR)_{16}(H_2O)_4]$ complexes. It consists of a central $[Mn_4^{IV}O_4]^{8+}$ cubane moiety, surrounded by an outer non-planar ring of eight Mn^{III} ions. The Jahn-Teller elongation axes on the Mn^{III} ions of complex **3a** are not all approximately perpendicular to the plane of the molecule (Mn_{12} core) as seen in other Mn_{12} complexes. The elongation axis on Mn6 is contained in the plane of the molecule. Fig. 3 (top) shows an ORTEP representation of complex **3a** emphasizing in black the Jahn-Teller elongation axes of the Mn^{III} ions.

Single crystals of $[Mn_{12}O_{12}(O_2CCH_2Bu^t)_{16}(H_2O)_4]\cdot CH_2Cl_2\cdot MeCN$ (**3b**) were obtained by recrystallizing from $CH_2Cl_2/MeCN$, the dried sample of **3a** that had converted to the HT form upon solvent loss over a period of several days. The purity of the HT form was checked by AC magnetic susceptibility measurements. Complex **3b** also crystallizes in the triclinic space group

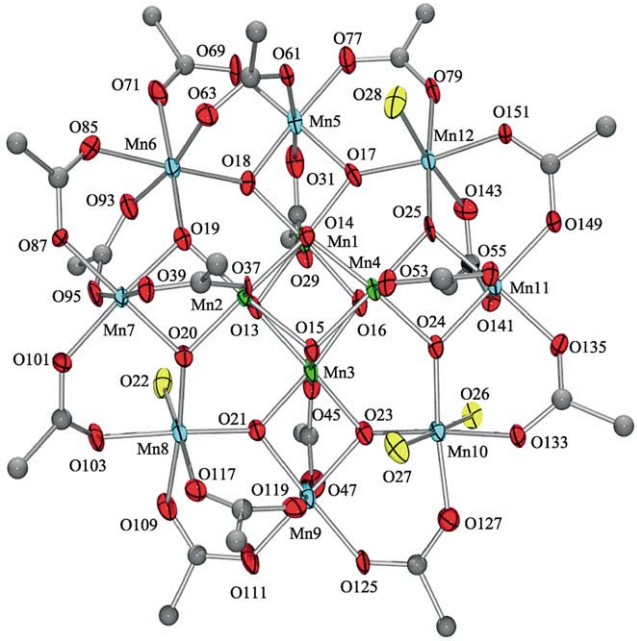

Fig. 2. PovRay plot of $[Mn_{12}O_{12}(O_2CCH_2Bu^t)_{16}(H_2O)_4]\cdot CH_2Cl_2\cdot MeNO_2$ (**3a**) at the 50% probability level, except for the C atoms. For clarity, only the α-C atom of the carboxylate *tert*-butylacetate groups are shown.

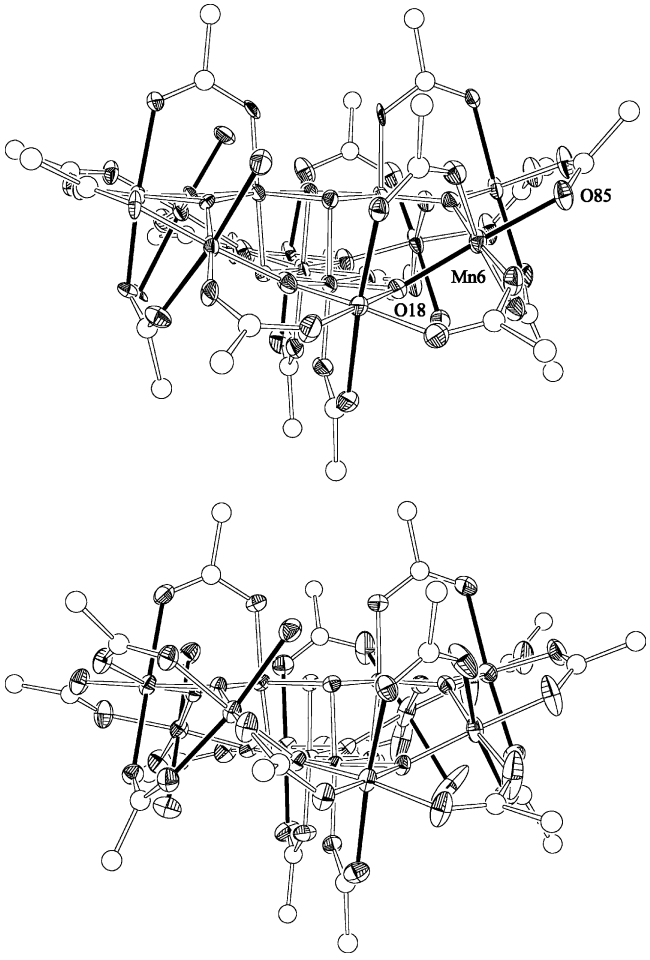

Fig. 3. ORTEP representation of $[Mn_{12}O_{12}(O_2CCH_2Bu^t)_{16}(H_2O)_4]\cdot CH_2Cl_2\cdot MeNO_2$ (**3a**) (top) and $[Mn_{12}O_{12}(O_2CCH_2Bu^t)_{16}(H_2O)_4]\cdot CH_2Cl_2\cdot MeCN$ (**3b**) (bottom) at the 50% probability level, except for the C atoms. For clarity, only the α-C atom of the carboxylate *tert*-butylacetate groups are shown. Jahn-Teller elongation axes are in bold.

$P\bar{1}$ and is isomorphous with **3a**. However, the $[Mn_{12}O_{12}(O_2CCH_2Bu^t)_{16}(H_2O)_4]$ molecule (Fig. 4) differs from that in complex **3a** in that all the JT elongation axes are approximately perpendicular to the plane of the molecule. The unit cell again contains two Mn_{12} molecules and two CH_2Cl_2 molecules, but in place of the two $MeNO_2$ molecules of **3a** there are two MeCN molecules in **3b**.

Apart from the difference in the orientation of one JT elongation axis (at Mn6 of **3a**), the two molecules are superimposable, as seen by comparing the cores of the molecules shown in Figs. 2 and 4. Fig. 5 shows the packing diagram of complexes **3a** and **3b**, respectively. In summary, the two JT isomers **3a** (LT) and **3b** (HT) crystallize in the same triclinic space group with analogous positions of their Mn_{12} and CH_2Cl_2 molecules, and differ only in that in **3a** where there is an $MeNO_2$ molecule, whereas in **3b** there is an MeCN at the same position.

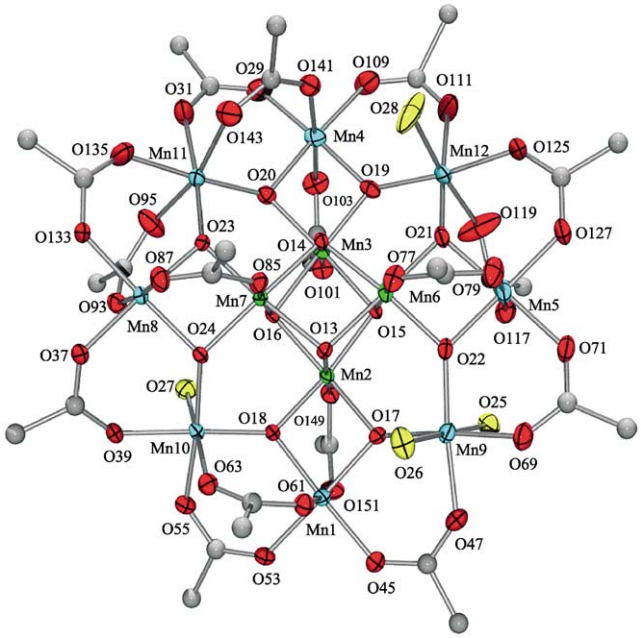

Fig. 4. PovRay plot of $[Mn_{12}O_{12}(O_2CCH_2Bu^t)_{16}(H_2O)_4]\cdot CH_2Cl_2\cdot MeCN$ (**3b**) at the 50% probability level, except for the C atoms. For clarity, only the α-C atom of the carboxylate *tert*-butylacetate groups are shown.

2.2. Magnetochemistry

Out-of-phase AC magnetic susceptibility signals (χ''_M) are seen for both complexes **3a** and **3b**. Fig. 6 shows a plot of χ''_M vs. T for complex **3a** (upper) and **3b** (lower) in the 2–10 K temperature range, measured at frequencies of 50, 250 and 997 Hz. Frequency-dependent χ''_M signals are a signature of an SMM. These complexes exhibit frequency-dependent χ''_M peaks, at 5–7 K for **3b** and at 2–4 K for **3a**.

The energy barriers for the reversal of the magnetization vector for the two forms of $[Mn_{12}O_{12}(O_2CCH_2Bu^t)_{16}(H_2O)_4]$ can be determined by analyzing the temperature of their χ''_M peak maxima at different frequencies. At the temperature of the χ''_M vs. T peak maximum, the relaxation rate equals the AC frequency (ν), and thus the relaxation rate ($1/\tau$) can be obtained from the relationship $\omega\tau = 1$, where $\omega = 2\pi\nu$. AC magnetic susceptibility data were collected at eight frequencies from 4.0 to 1488 Hz, plotted as $\ln(1/\tau)$ vs. $1/T$, and fit to the Arrhenius equation. Relaxation data at even lower temperatures were obtained from DC relaxation decay measurements on single crystals of **3a** and **3b** using a micro-SQUID apparatus. The combined AC and DC data for complexes **3a** and **3b** and the fits to the Arrhenius equation (solid lines) are shown in Fig. 7. The HT form (complex **3b**) has an effective energy barrier (U_{eff}) of 62 K with $1/\tau_o = 4.2 \times 10^7\ s^{-1}$, whereas the LT form (complex **3a**) has a smaller U_{eff} of 42 K with $1/\tau_o = 4.5 \times 10^9\ s^{-1}$. These parameters are similar

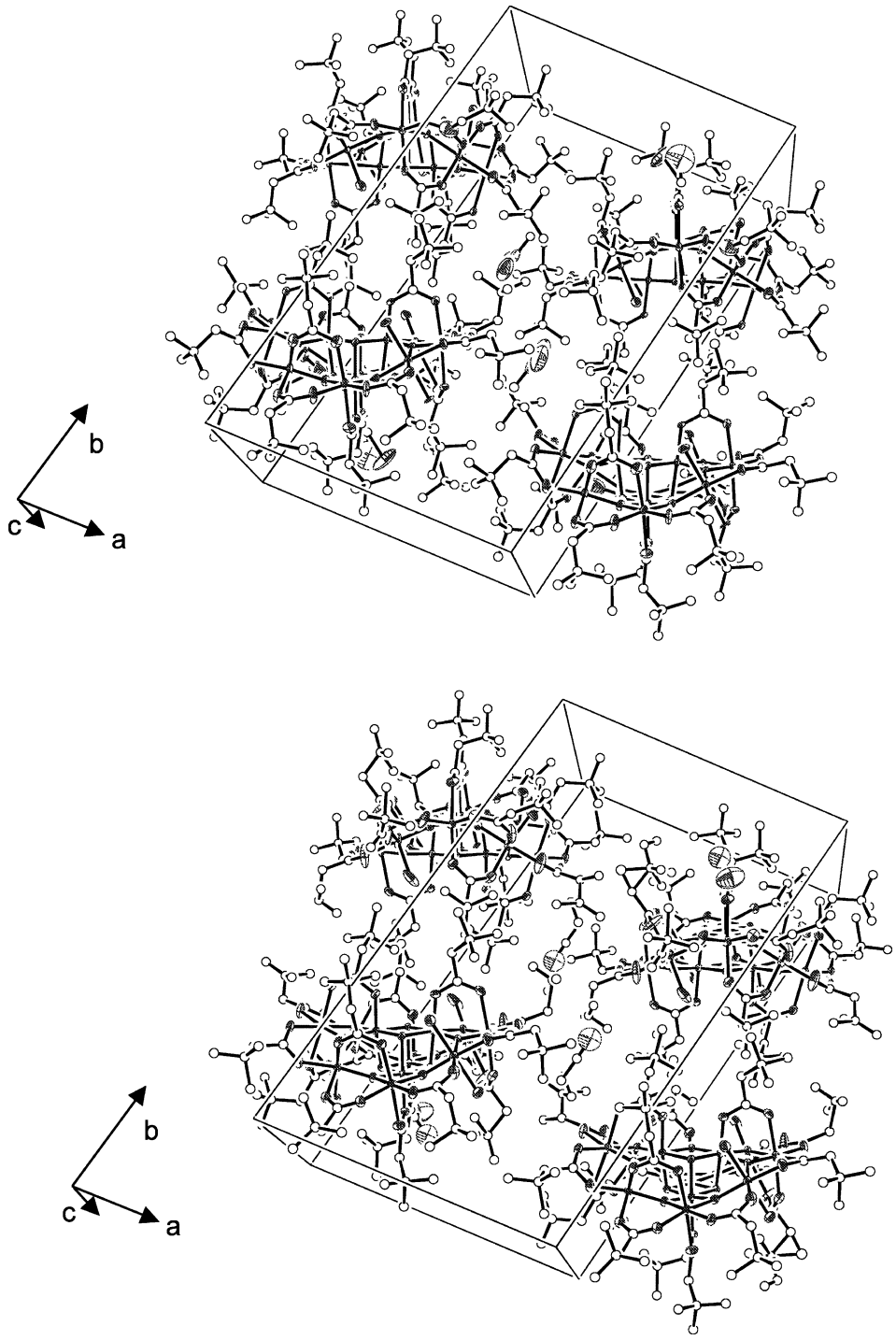

Fig. 5. Molecular packing of **3a**·CH_2Cl_2·$MeNO_2$ (top) and **3b**·CH_2Cl_2·MeCN (bottom). Hydrogen atoms are omitted for clarity.

to the ones obtained for the other pair of Jahn-Teller isomers, complexes **2a** and **2b**. In that case, the HT form had $U_{eff} = 64$ K and $1/\tau_o = 1.2 \times 10^8$ s^{-1} and the LT form had $U_{eff} = 38$ K with $1/\tau_o = 5.0 \times 10^9$ s^{-1}.

Magnetization vs. DC field scans were performed on aligned crystals of **3a** and **3b** using a micro-SQUID apparatus, and the resulting hysteresis loops at low temperatures are shown in Fig. 8. Complex **3a** was measured at temperatures < 1.8 K and a 0.008 T s^{-1} sweep rate, and complex **3b** at temperatures < 4.4 K and a 0.14 T s^{-1} sweep rate. Both **3a** and **3b** display clear hysteresis with coercivities that vary with temperature, as expected for SMMs. The hysteresis loops are not smooth, but instead show the steps those are the signature of QTM. The field separation between steps (ΔH), which can best be determined from the first

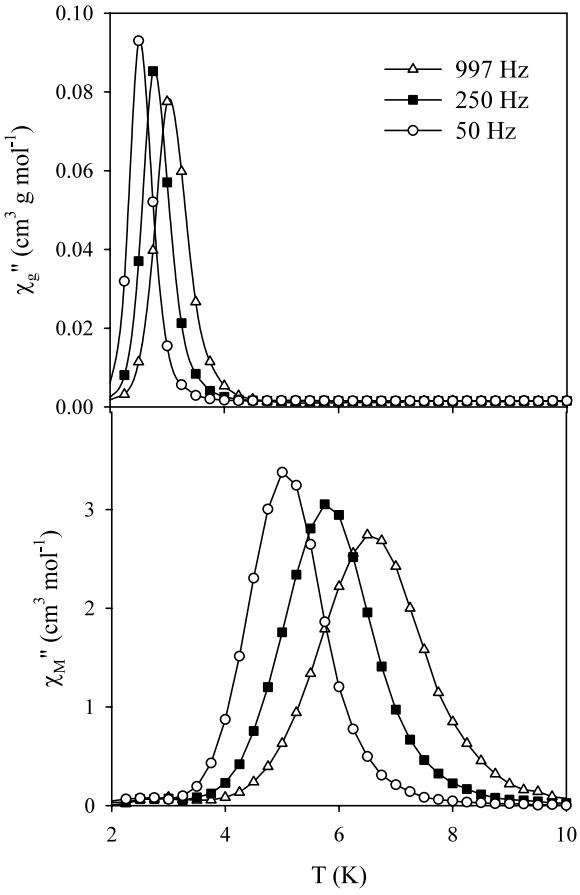

Fig. 6. Out-of-phase AC magnetic susceptibility plots for $[Mn_{12}O_{12}(O_2CCH_2Bu^t)_{16}(H_2O)_4]$ molecule; **3a**·CH_2Cl_2·$MeNO_2$·(top) and **3b**·CH_2Cl_2·MeCN (bottom), at the indicated frequencies.

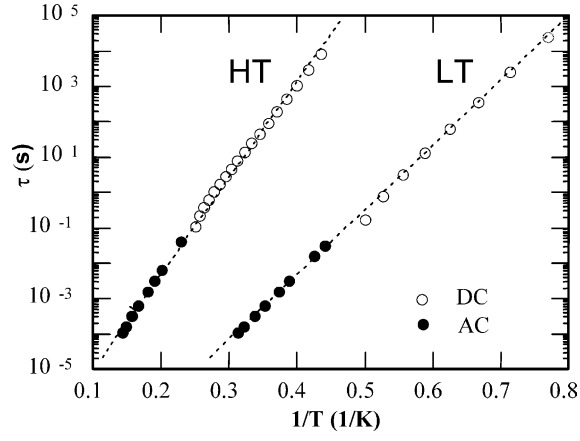

Fig. 7. Plots of relaxation time (τ) vs. $1/T$ for complexes **3a** (LT form) and **3b** (HT form) using AC χ''_M data and DC magnetization decay data. The solid lines are fits to the Arrhenius equation. See text for the fitting parameters.

derivative of the hysteresis loop, is proportional to D. Measurement of the step positions for complex **3b** in Fig. 8 gave an average ΔH of 0.45 T (4.5 kG). This gives a $|D|/g$ value of 0.21 cm^{-1} for **3b** and $D = -0.42$ cm^{-1}

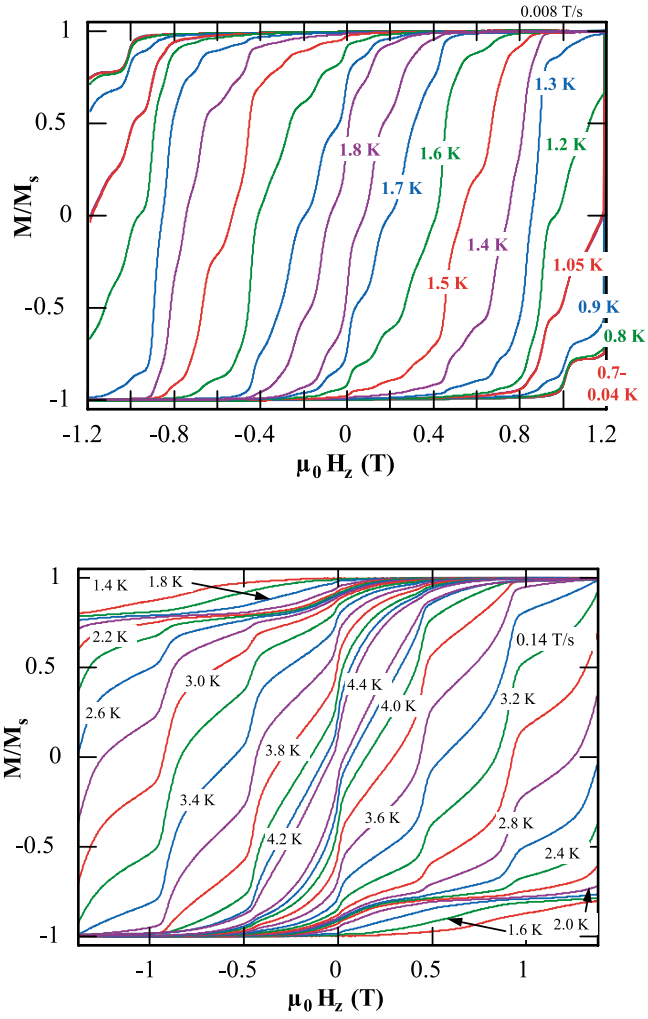

Fig. 8. Magnetization hysteresis loop for complex **3a** in the 1.8–0.04 K temperature range at a 0.008 T s^{-1} field sweep rate (top). Magnetization hysteresis loop for complex **3b** in the 4.4–1.4 K range at 0.14 T s^{-1} sweep rate (bottom).

for $g = 2$. This gives $U = S^2|D| = 61$ K, as expected for neutral Mn_{12} complexes. In the case of complex **3a**, the value of $|D|/g$ is not so straightforward to calculate, and further studies are in progress.

3. Conclusions

Two crystal structures of $[Mn_{12}O_{12}(O_2CCH_2Bu^t)_{16}(H_2O)_4]$ (**3**) have been obtained, **3**·CH_2Cl_2·$MeNO_2$ (**3a**) and **3**·CH_2Cl_2·MeCN (**3b**). The two complexes exhibit two different relaxation rates of the magnetization, with out-of-phase (χ''_M) peaks in the 2–4 K region for complex **3a** (LT form) and out-of-phase (χ''_M) peaks in the 5–7 K range for complex **3b** (HT form). The LT form has smaller U_{eff} than the HT form. This is consistent with the fact that complex **3a** has one Jahn-Teller elongation axis oriented perpendicular to the easy axis of the molecule, rather than having, as in

complex **3b**, all the Jahn-Teller elongation axis approximately parallel to each other and approximately parallel to the easy axis of the molecule. Apart from this difference, both crystal structures are very similar, and only differ in the identity of one solvent of crystallization. Thus the two JT isomers are stabilized by relatively small differences in the environment, suggesting very small energy differences between them.

Acknowledgements

This work was supported by the National Science Foundation.

References

[1] (a) R. Sessoli, H.-L. Tsai, A.R. Schake, S. Wang, J.B. Vincent, K. Folting, D. Gatteschi, G. Christou, D.N. Hendrickson, J. Am. Chem. Soc. 115 (1993) 1804;
(b) R. Sessoli, D. Gatteschi, A. Caneschi, M.A. Novak, Nature 356 (1993) 141;
(c) G. Christou, D. Gatteschi, D.N. Hendrickson, R. Sessoli, MRS Bull. 25 (2000) 66.

[2] (a) J.R. Friedman, M.P. Sarachik, J. Tejada, R. Ziolo, Phys. Rev. Lett. 76 (1996) 3830;
(b) L. Thomas, L. Lionti, R. Ballou, D. Gatteschi, R. Sessoli, B. Barbara, Nature 383 (1996) 145;
(c) J. Tejada, R.F. Ziolo, X.X. Zhang, Chem. Mater. 8 (1996) 1784.

[3] Z. Sun, D. Ruiz, N.R. Dilley, M. Soler, J. Ribas, K. Folting, M.B. Maple, G. Christou, D.N. Hendrickson, Chem. Commun. (1999) 1973.

[4] (a) S.M.J. Aubin, Z. Sun, H.J. Eppley, E.M. Rumberger, I.A. Guzei, K. Folting, P.K. Gantzel, A.L. Rheingold, G. Christou, D.N. Hendrickson, Inorg. Chem. 40 (2001) 2127;
(b) M.J. Aubin, Z. Sun, H.J. Eppley, E.M. Rumberger, I.A. Guzei, K. Folting, P.K. Gantzel, A.L. Rheingold, G. Christou, D.N. Hendrickson, Polyhedron 20 (2001) 1139.

[5] H.J. Eppley, H.-L. Tsai, N. de Vries, K. Folting, G. Christou, D.N. Hendrickson, J. Am. Chem. Soc. 117 (1995) 301.